Mitochondrial Nitric Oxide Synthase Drives Redox Signals for Proliferation and Quiescence in Rat Liver Development

María C. Carreras,[1,2] Daniela P. Converso,[1] Alicia S. Lorenti,[3] Mariana Barbich,[3] Damián M. Levisman,[1] Ariel Jaitovich,[1] Valeria G. Antico Arciuch,[1] Soledad Galli,[1] and Juan J. Poderoso[1]

Mitochondrial nitric oxide synthase (mtNOS) is a fine regulator of oxygen uptake and reactive oxygen species that eventually modulates the activity of regulatory proteins and cell cycle progression. From this perspective, we examined liver mtNOS modulation and mitochondrial redox changes in developing rats from embryonic days 17–19 and postnatal day 2 (proliferating hepatocyte phenotype) through postnatal days 15–90 (quiescent phenotype). mtNOS expression and activity were almost undetectable in fetal liver, and progressively increased after birth by tenfold up to adult stage. NO-dependent mitochondrial hydrogen peroxide (H_2O_2) production and Mn-superoxide dismutase followed the developmental modulation of mtNOS and contributed to parallel variations of cytosolic H_2O_2 concentration ($[H_2O_2]_{ss}$) and cell fluorescence. mtNOS-dependent $[H_2O_2]_{ss}$ was a good predictor of extracellular signal–regulated kinase (ERK)/p38 activity ratio, cyclin D1, and tissue proliferation. At low 10^{-11}–10^{-12} M $[H_2O_2]_{ss}$, proliferating phenotypes had high cyclin D1 and phospho-ERK1/2 and low phospho-p38 mitogen-activated protein kinase, while at 10^{-9} M $[H_2O_2]_{ss}$, quiescent phenotypes had the opposite pattern. Accordingly, leading postnatal day 2–isolated hepatocytes to embryo or adult redox conditions with H_2O_2 or NO-H_2O_2 scavengers, or with ERK inhibitor U0126, p38 inhibitor SB202190 or p38 activator anisomycin resulted in correlative changes of ERK/p38 activity ratio, cyclin D1 expression, and [^{3}H] thymidine incorporation in the cells. Accordingly, p38 inhibitor SB202190 or N-acetylcysteine prevented H_2O_2 inhibitory effects on proliferation. In conclusion, the results suggest that a synchronized increase of mtNOS and derived H_2O_2 operate on hepatocyte signaling pathways to support the liver developmental transition from proliferation to quiescence. (HEPATOLOGY **2004;40:157–166.**)

Abbreviations: mtNOS, mitochondrial nitric oxide synthase; ERK, extracellular signal–regulated kinase; Mn-SOD, manganese superoxide dismutase; NOS, nitric oxide synthase; MAPK, mitogen-activated protein kinase; PMSF, phenylmethylsulfonyl fluoride; L-NMMA, N^G-methyl-L-arginine; iNOS, inducible nitric oxide synthase; nNOS, neuronal nitric oxide synthase; eNOS, endothelial nitric oxide synthase; FCS, fetal calf serum; UQ, ubiquinone; NAC, N-acetyl-cysteine.

From the [1]Laboratory of Oxygen Metabolism, University Hospital and the [2]Department of Clinical Biochemistry, School of Pharmacy and Biochemistry, University of Buenos Aires, Buenos Aires, Argentina; and [3]Instituto de Ciencias Básicas y Medicina Experimental, Hospital Italiano, Buenos Aires, Argentina.

Received November 17, 2003; accepted March 24, 2004.

Supported by the University of Buenos Aires (UBACyT M627), the National Agency for Promotion of Scientific and Technological Development (PICT 08468), Consico Nacional de Investigaciones Cientificas y Técnicas (PIP 58), and Fundación Pérez Companc, Buenos Aires, Argentina.

Address reprint requests to: Professor María Cecilia Carreras, Ph.D., Laboratory of Oxygen Metabolism,University Hospital, Córdoba 2351, 1120 Buenos Aires, Argentina. E-mail: carreras@ffyb.uba.ar; fax: 54-11-59508811.

Published online in Wiley InterScience (www.interscience.wiley.com).

DOI 10.1002/hep.20255

In normal adult liver, hepatocytes are highly differentiated and rarely undergo cell division, but they retain a remarkable ability to proliferate in response to acute or chronic injury.[1] While liver regeneration depends on the transcriptional effects of cytokines, the mechanisms that govern developmental hepatocyte proliferation and the transition to the quiescent condition are not fully characterized.

At relatively low matrix steady-state concentration, NO exerts marked inhibitory effects on the activity of redox components of the electron transfer chain, particularly on cytochrome oxidase, thus regulating oxygen uptake.[2,3] Consequently, the reduction level of mitochondrial components increases on the substrate side, leading to high superoxide anion (O_2^-) production[4]; most of O_2^- is dismutated by matrix manganese superoxide dismutase (Mn-SOD) to hydrogen peroxide (H_2O_2) that freely diffuses outside the mitochondria.

Nitric oxide is vectorially released into matrix by mitochondrial nitric oxide synthases (mtNOSs). Different mtNOS isoforms have been described in rat tissues[5–7]; liver mtNOS is a Ca^{2+}/calmodulin-dependent, constitutively expressed variant that is localized in the inner mitochondrial membrane. Elfering et al. reported 100% homology between liver mtNOS and neuronal nitric oxide synthase (NOS)-α by mass spectrometry[8]; differentially, liver mtNOS has two posttranslational modifications: acylation with myristic acid and phosphorylation at C terminus, and a lower molecular weight (130 vs. 157 kDa). Additionally, mtNOS is subjected to selective modulation by thyroid status,[3] cold acclimation,[9] hypoxia,[10] and brain plasticity.[11]

Hydrogen peroxide and the consequent oxidative stress level play an important role in the activation of signaling molecules that control the complex machinery involved in cell proliferation, differentiation, apoptosis, and senescence.[12] The major components of the cell cycle machinery are the cyclins and cyclin-dependent kinases. Cyclin D1 is implicated in the control of G1 phase progression in hepatocytes and other proliferating cell types,[13] and its expression is positively regulated by the extracellular signal–regulated kinase (ERK) pathway and antagonized by stress-activated p38 mitogen-activated protein kinase (MAPK) cascade.[14] During liver development, cyclin D1 content is inversely related to p38 MAPK activity,[15] which in turn may be regulated by reactive oxygen species[16,17] and NO.[18,19]

Considering the mitochondrial utilization of NO and the NO-derived production of oxygen-active species, the regulation of mtNOS provides new insight into the physiological significance of mitochondria in cell biology. We report the modulation of mtNOS activity and the putative regulation of cell cycle redox signaling in the sequence of proliferating to quiescent cell stages during rat liver development.

Materials and Methods

Animals. Wistar rats were used in the experiments. National Research Council criteria for the care and use of laboratory animals in research were followed.

Preparation of Whole Liver Homogenates. Pooled liver of one litter from fetal (embryonic days 17 [E17] and 19 [E19]) and newborn rats at postnatal day 2 (P2), or whole liver of young and adult rats (P15–P90) were homogenized in 1 mL of cold lysis buffer (50 mM HEPES [pH 7.5], 150 mM NaCl, 1 mM ethylenediaminetetraacetic acid (EDTA), 2.5 mM ethyleneglycol tetraacetic acid [EGTA], 1 mM dithiothreitol, 10% glycerol, 1 mM phenylmethylsulfonyl fluoride [PMSF], 10 μg/mL each of aprotinin and leupeptin, 50 mM NaF and 0.1 mM sodium orthovanadate) per 100 mg of tissue.[14] Tween 20 was then added at a final concentration of 0.1%. Homogenates were clarified by centrifugation at 10,000*g* for 10 minutes at 4°C and stored at −70°C.

Isolation and Purification of Liver Mitochondria. Liver was homogenized in MSHE buffer (225 mM mannitol, 70 mM sucrose, 1 mM EGTA, 25 mM HEPES), pH 7.4 with 5 μg/mL each of aprotinin and leupeptin, 100 μg/mL PMSF, 10 μg/mL pepstatin, and 0.1% bovine serum albumin. The homogenate was centrifuged at 700*g* at 4°C for 10 minutes; the supernatant was centrifuged at 7000*g* for 10 minutes.[3] A mitochondrial pellet was further purified using Percoll gradient to completely remove contaminating organelles and broken mitochondria. Purified mitochondria were tested for contamination by comparing lactate dehydrogenase activity (cytosolic marker) to succinate-cytochrome *c* reductase activity (mitochondrial marker); minimal contamination was found (2%–5%).

Mitochondrial Enzyme Activities. Nicotinamide adenine dinucleotide– and succinate-cytochrome *c* reductase activities (complexes I-III and II-III, respectively) were assayed by cytochrome *c* reduction at 550 nm with a Hitachi U3000 spectrophotometer (Hitachi, Tokyo, Japan) at 30°C. Cytochrome oxidase activity (complex IV) was determined by monitoring cytochrome *c* oxidation at 550 nm ($\epsilon_{550} = 21\ mM^{-1} \cdot cm^{-1}$); the reaction rate was measured as the pseudo-first order reaction constant (k') and expressed as k'/min · mg protein. [20]

NOS Activity. NOS activity was determined through the conversion of [^{3}H]-L-arginine to [^{3}H]-L-citrulline in 50 mM of potassium phosphate buffer (pH 7.5) in the presence of 100 μM L-arginine, 0.1 μM [^{3}H]-L-arginine (NEN, Boston, MA), 0.1 mM NADPH, 0.3 mM $CaCl_2$, 0.1 μM calmodulin, 10 μM tetrahydrobiopterin, 1 μM flavin adenine dinucleotide, 1 μM flavin mononucleotide, 50 mM L-valine and 1 mg/ml protein.[3] Specific activity was calculated by subtracting the remaining activity in the presence of the NOS inhibitor N^G-methyl-L-arginine (5 mM L-NMMA) or 2 mM EGTA.

Immunoblotting. Cells were disrupted in lysis buffer (50 mM Tris buffer [pH 7.4]; 0.5% Nonidet P-40; 150 mM NaCl; 1 mM EDTA; 1 mM EGTA; 10% glycerol; 1 mM $MgCl_2$; 1 mM PMSF; 5 μg/mL each of aprotinin, leupeptin, and pepstatin; 1 mM sodium orthovanadate; 25 mM NaF; and 0.1 mM ammonium molybdate). Lysates were centrifuged at 12,000*g* for 30 minutes at 4°C, and the supernatants were stored at −70°C. Western blot analysis was performed as described[11]; membranes were stained with Ponceau red to ensure equivalent amounts of protein loading and electrophoretic transfer among sam-

ples. Western blotting enhanced chemiluminescence detection system and Hybond-P membranes were from Amersham Biosciences (Little Chalfont, United Kingdom). Quantification of bands was performed using digital image analysis (Total Lab, Nonlinear Dynamics, Newcastle, UK). Liver homogenates of lipopolysaccharide-treated rats, cerebellum cytosol, and endothelial cell lysates were used as inducible nitric oxide synthase (iNOS)-, neuronal nitric oxide synthase (nNOS)-, and endothelial nitric oxide synthase (eNOS)-positive controls. Proliferating liver from rats treated with a single dose of T3 (60 μg/100 g body weight, intraperitoneally) was used as a control for signaling assays.[21]

Co-immunoprecipitation. Mitochondrial or cytosolic proteins (500 μg) were incubated with 4 μg of polyclonal nNOS antibody and 30 μL protein A/G PLUS-Agarose (Santa Cruz, CA) at 4°C. The beads were then washed three times, suspended in sample buffer, boiled, and centrifuged, and the supernatants were subjected to immunoblotting against monoclonal nNOS antibodies.

Antibodies. Polyclonal anti-iNOS and anti-nNOS, anti-cyclin D2 and D3, and monoclonal anti–mouse cyclin D1 were obtained from Santa Cruz Biotechnology, Inc. (Santa Cruz, CA); polyclonal anti-eNOS and monoclonal nNOS antibodies were obtained from Transduction Laboratories (Lexington, KY). Polyclonal antibodies against total and phospho-p38 MAPK, ERK ½ and c-Jun N-terminal kinase, and phospho–MAPK kinases ½ were from Cell Signaling Technology (Beverly, MA).

Immunoelectron Microscopy. Purified mitochondria were suspended in 4% formaldehyde (pH 7.4) for 2 hours at 4°C, then dehydrated in 70%, 96%, and 100% ethanol (30 minutes for each step) and embedded in LR White. Immunocytochemistry was performed using a primary mouse anti–C-terminal nNOS (1095-1289) at a dilution of 1:100 in phosphate-buffered saline (pH 7.4). Grids were washed in phosphate-buffered saline and counterstained with 1% uranyl acetate. Nonspecific background was blocked by incubation with 5% normal goat serum in phosphate-buffered saline at the beginning of the procedure. Specimens were observed in a Zeiss EM-109-T transmission electron microscope at 80 kv.

Mitochondrial H_2O_2 Production. H_2O_2 production was continuously monitored using a Hitachi F-2000 spectrofluorometer (Hitachi) with excitation and emission wavelengths at 315 and 425 nm, respectively.[22] The reaction medium, which consisted of potassium phosphate buffer (50 mM) and 50 mM L-valine, was supplemented with 10 mM succinate, 12.5 units/mL horseradish peroxidase, 250 μM *p*-hydroxyphenyl-acetic acid, and 0.15 mg of mitochondrial protein per mL. NO-dependent H_2O_2 production was determined as the difference of H_2O_2 production rate in the presence of 100 μM L-arginine and L-arginine plus 2 mM L-NMMA. Mitochondrial preparations were supplemented with 1 μM Mn(III)tetrakis(4-benzoic acid) porphyrin (Cayman Chemical, Ann Arbor, MI) to uniform the maximal H_2O_2 production rate.

Cell Isolation and Culture. Hepatocytes were isolated by collagenase digestion as described previously.[23] For culture, P2- and P15-isolated hepatocytes were seeded in 96-well plates (50,000 cells per well) in medium 199 (Gibco-BRL, Invitrogen Life Technologies, Breda, the Netherlands) supplemented with 10% fetal calf serum (FCS) and 50 μg/mL gentamicin and were allowed to attach for 4 hours. Cells were synchronized by 20-hour incubation with 2% FCS and 2 hours without FCS. Hepatocyte treatments were performed in medium 199 with 10% FCS for 72 hours. Proliferation was assayed through [^{3}H] thymidine incorporation.[11] The last 24 hours, cells were incubated with 0.8 μCi[^{3}H] thymidine/well and harvested; cpm were measured in a liquid scintillation counter (Wallac 1414, Turku, Finland).

Detection of Intracellular ROS. Intracellular ROS were analyzed by flow cytometry, using a 2′,7′-dichlorofluorescin diacetate probe. [23] The cellular fluorescence intensity was measured after 30 minutes of incubation with 5 μM 2′,7′-dichlorofluorescin diacetate by using an Ortho Cytoron Absolute Flow-Cytometer (Johnson & Johnson, Raritan, NY). Propidium iodide (0.005%) was used to detect dead cells. For each analysis, 10,000 events were recorded.

DNA Analysis. For measuring apoptosis, the ploidy determination of hepatocytes was assessed with propidium iodide staining and flow cytometry as described previously.[24]

Antioxidant Enzyme Activities. Mitochondrial Mn-SOD activity was determined by inhibition of cytochrome *c* reduction at 550 nm in 50 mM potassium phosphate buffer/0.1 mM EDTA (pH 7.8) at 25°C.[25] Catalase and glutathione peroxidase activities in 7,000*g* supernatants were determined by the decrease in H_2O_2 absorption at 240 nm ($\epsilon_{240} = 41\ \mu M^{-1} \cdot cm^{-1}$), [26] or by the oxidation of NADPH at 340 nm ($\epsilon_{340} = 6.22\ mM^{-1} \cdot cm^{-1}$).[27]

Reagents. SDS, glycerol, 2-(β-mercaptoethanol), and bromophenol blue were obtained from Bio-Rad (Richmond, CA); SB 202190 was obtained from Calbiochem (San Diego, CA); U0126 was obtained from Cell Signaling Technology; and other chemicals were from Sigma Chemical Co. (St Louis, MO).

Data Analysis. Data are expressed as mean ± SE and were analyzed by ANOVA and Scheffé test. Simple linear

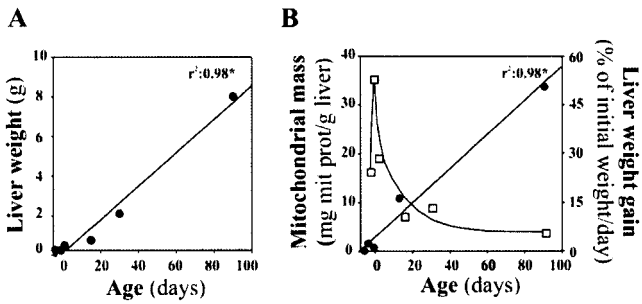

Fig. 1. Liver weight and mitochondrial mass variations during rat liver development. (A) Progression of total liver weight with age. (B) Developmental ages are plotted with the rate of liver weight gain (□), and the respective mitochondrial mass (●). mit prot, mitochondrial protein.

regression was utilized as appropriate. Statistical significance was accepted at $P < .05$.

Results and Discussion

Mitochondrial Maturation in Rat Liver Development. Liver mass continuously increases with age due to cell duplication and hypertrophy (Fig. 1A).[28] From E19 to adulthood, relative liver weight went from 6.1% to 3.4% of body weight and liver growth decreased tenfold (Fig. 1B). Likewise, transition from fetal to adult liver is accompanied by a burst of hepatocyte proliferation in late gestation and in the immediate neonatal period (E19–P2–3), followed by a decrease of proliferation after the first postnatal week.[13] Instead, mitochondrial biogenesis is persistently active throughout development; mitochondrial protein content increased from 0.13 (E19) to 34 mg per g of liver tissue (P90) (Fig. 1B). To evaluate mitochondrial maturation, enzyme activities were tested in the same conditions. Mitochondria isolated from maximally proliferating liver at E19–P2 retained 40%–50% of complex I, II-III, and IV activities of quiescent organelles; mitochondrial ubiquinone (UQ) had a similar pattern (Table 1). Previous reports showed an increase of the specific activity of a number of oxidative enzymes during the early postnatal development.[29] Both increasing mitochondrial pool and phenotypic changes may take part in the sequential proliferating–differentiating process.[30] It is surmised that promotion of proliferation requires a controlled inhibition of mitochondrial respiration[31]; specifically, low complex activities and reduced mitochondrial mass have a negative impact on redox mitochondrial-dependent cell signaling.

Mitochondrial NOS Is Modulated During Development. The increase or decrease of mtNOS content can be an adaptive mechanism to control mitochondrial functions.[3,9] In this study, liver mtNOS content was clearly modulated during rat development: it was almost undetectable at highly proliferative E19, while it progressively increased after birth, up to quiescent P30–P90 (Fig. 2A); modulation was confirmed by immunoelectron microscopy (Fig. 2E). mtNOS activity paralleled protein expression—both increased tenfold from fetal to adult stages (Fig. 2A and B). Considering the variations of mitochondrial mass, mtNOS activity per gram of liver tissue enhanced in the adult organ by 500-fold. It is then inferred that, during liver development, (1) matrix NO steady-state concentration raises by sequential increase of mtNOS content and (2) total NO liver production is greatly amplified by the expansion of the mitochondrial pool.

Although it is a nNOS variant,[3,8] 130-kDa liver mtNOS reacts with both anti-nNOS and anti-iNOS antibodies (see Fig. 2A); eNOS was not detected in liver mitochondria. Interestingly, cytosol immunoblotting with antibodies against nNOS revealed two specific bands: classic nNOS-α with M_r of 157 kDa and a second band with 130 kDa, the expression of which was inversely modulated. The specificity of the nNOS 130-kDa band variant was validated by immunoprecipitation of mitochondria and cytosolic proteins from P2 liver (see Fig. 2B). Moreover, 130-kDa protein was solely evidenced at early stages while, concomitantly with a higher expression of mtNOS, it disappeared from cytosol after P15. This pattern suggests that cytosol 130-kDa protein is the enzyme translocated to mitochondria during development. Comparatively, cytosolic NOS activity, as contributed by the Ca-dependent isoforms, increased early at birth and remained stable up to adult stage; no significant modulation of

Table 1. Mitochondrial Enzyme Activities and Ubiquinol Content in Rat Liver Development

	E19	P2	P15	P30	P90
Complexes I–III (nmol/min.mg prot)	170 ± 28*	247 ± 68*	404 ± 54	417 ± 27	441 ± 52
Complexes II–III (nmol/min.mg prot)	37 ± 7*	48 ± 6*	55 ± 6*	89 ± 9	96 ± 10
Complex IV (k′/min.mg prot)	5 ± 1*	11 ± 1*	14 ± 1	17 ± 2	16 ± 2
UQ-9 content (nmol/mg prot)	ND	1.1 ± 0.1*	2 ± 0.1	1.8 ± 0.1	1.9 ± 0.1

Abbreviations: E, embryonic; P, postnatal; prot, protein; UQ, ubiquinone; ND, not determined.

NOTE: Complexes I–III: NADH-cytochrome *c* reductase. Complexes II–III: succinate-cytochrome *c* reductase. Complex IV: cytochrome oxidase. Data are expressed as mean ± SE from 4–8 different experiments.

*$P < .05$ respect to P90.

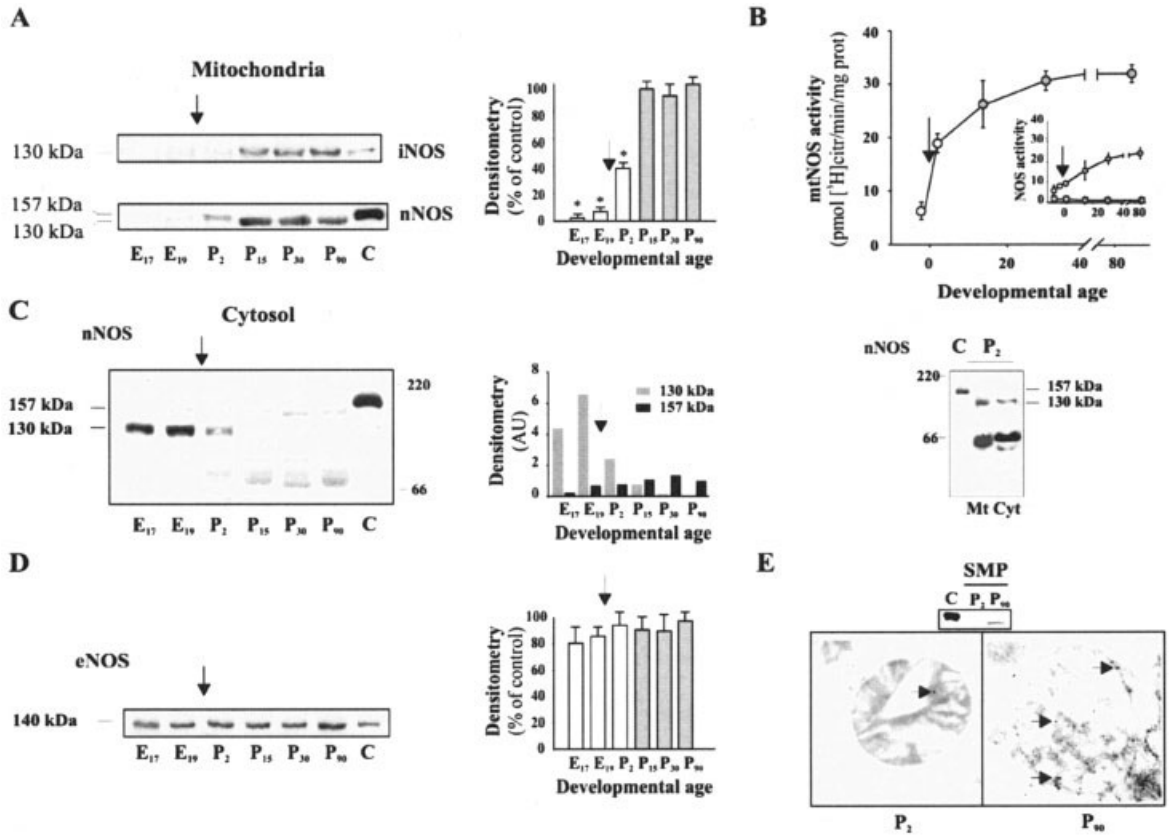

Fig. 2. Modulation of mitochondrial and cytosolic NOS during liver development. Proteins (50 μg/lane) were separated in 7.5% gels. (A) Left, mtNOS expression in embryonic and postnatal mitochondria with anti-iNOS and anti-nNOS antibodies; right, densitometry of mtNOS (anti-nNOS; P90 value was set as 1). (B) mtNOS activity as measured by the conversion of [^{3}H]-L-arginine to [^{3}H]-L-citrulline. Inset: cytosolic Ca^{2+}-dependent (○) and independent (□) NOS activities. (C) Left, cytosol immunoblotting with anti-nNOS; center, relative expression of nNOS variants; right, co-immunoprecipitation of mitochondrial and cytosolic proteins of P2 livers with polyclonal nNOS antibodies. (D) Cytosol immunoblotting with anti-eNOS antibodies. Data are mean ± SE of three separate experiments. White columns represent proliferating phenotypes; grey columns represent quiescent phenotypes. *$P < .05$ versus P90. (E) Immunoelectron microscopy of isolated purified liver mitochondria from P2 and adult rats. The organelles were labeled with anti-nNOS antibody and treated with a goat anti–mouse serum conjugated with colloidal gold (10-nm diameter particles). (Original magnification ×85,000.) Inset: mtNOS in submitochondrial particles from the same organelles. iNOS, inducible nitric oxide synthase; nNOS, neuronal nitric oxide synthase; E, embryonic; P, postnatal; mtNOS, mitochondrial nitric oxide synthase; [^{3}H]citr, [^{3}H]-L-citrulline; prot, protein; NOS, nitric oxide synthase; Mt, mitochondria; Cyt, cytosol; SMP, submitochondrial particles.

eNOS expression was detected (Fig. 2B [inset] and D).

The selective mtNOS modulation could be related to developmental activities of membrane mitochondrial transporters and chaperone proteins, or to enzyme activation or degradation. It has been reported that arginase[32] and calpain proteases[33] are higher in fetal liver than in adult liver, contributing to low matrix NO levels in fetal hepatocytes by reducing NOS substrate and/or by increasing mtNOS degradation by mitochondrial calpains.

mtNOS Modulation Correlates With Liver Mitochondrial Hydrogen Peroxide Yield. Immature mitochondria supplemented with complex III inhibitor antimycin had a noticeably slower H_2O_2 production rate than adult organelles (Fig. 3A). According to Table 1, respiratory chain activities per unit of mitochondrial protein increases with developmental age, possibly accounting for the decreased H_2O_2 production rate in less mature mitochondria.

In a physiological setting, supplementation of mitochondria with NO promotes a significant O_2^- burst[4]; NO inhibits cytochrome oxidase and *b-c*1 region at complex III and increases the ubisemiquinone radical level that provides the electrons to O_2.[22] Mitochondrial production of freely diffusible H_2O_2 depends on superoxide dismutase–catalyzed dismutation of NO-dependent O_2^- (reaction [3]):

$$NO + UQH^- \rightarrow NO^- + UQ^- + H^+ \quad (1)$$

$$UQ^- + O_2 \rightarrow UQ + O_2^- \quad (2)$$

$$2O_2^- + 2H^+ \xrightarrow{\text{Mn-SOD}} H_2O_2 + O_2 \quad (3)$$

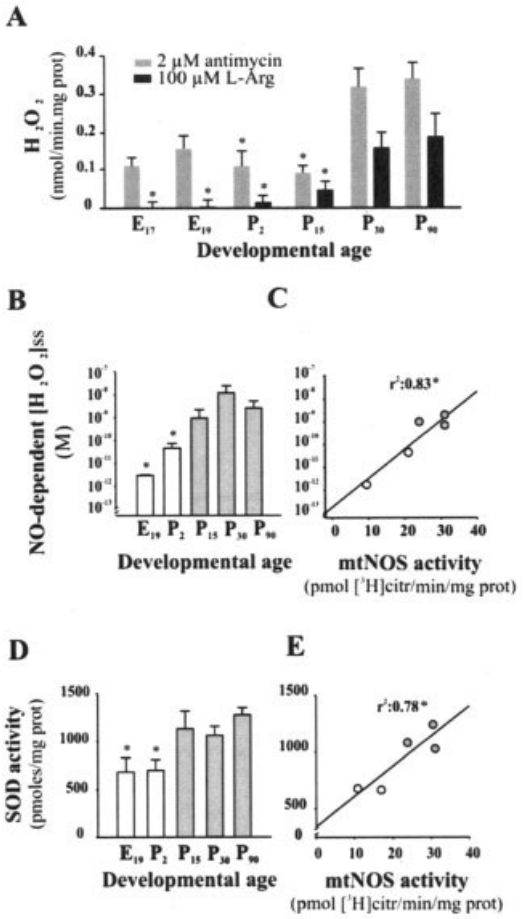

Fig. 3. Effect of mtNOS modulation on mitochondrial H_2O_2 production. (A) NO-dependent H_2O_2 production rate is compared with maximal H_2O_2 production rate with antimycin. (B) NO-dependent hydrogen peroxide steady-state concentration ($[H_2O_2]_{ss}$) as in the equation noted in Results. (C) Simple linear regression between cytosol $[H_2O_2]_{ss}$ and mtNOS activity. (D) Modulation of Mn-SOD activity during rat liver development; (E) correlation with mtNOS. White columns or circles represent proliferating phenotypes; grey columns or circles represent quiescent phenotypes. *$P < .05$ versus P90. Data represent 4–8 samples from each group. prot, protein; L-Arg, L-arginine; iNOS, inducible nitric oxide synthase; E, embryonic; P, postnatal; mtNOS, mitochondrial nitric oxide synthase; SOD, superoxide dismutase; [3H]citr, [3H]-L-citrulline.

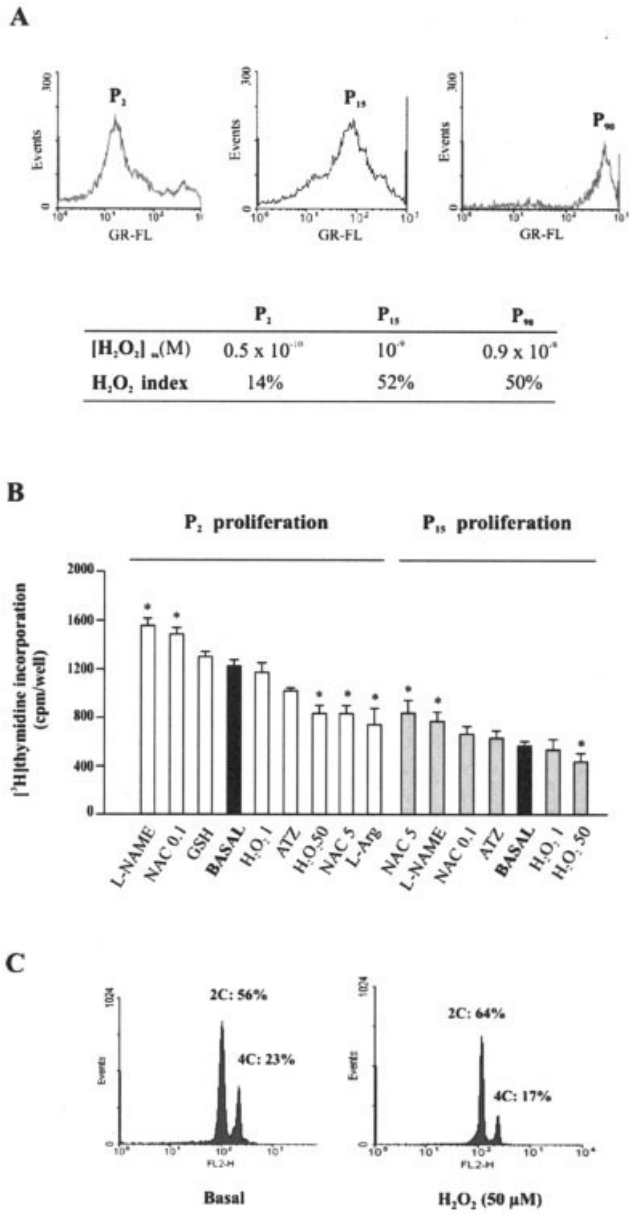

	P2	P15	P90
$[H_2O_2]_{ss}$(M)	0.5×10^{-10}	10^{-9}	0.9×10^{-9}
H_2O_2 index	14%	52%	50%

Fig. 4. Developmental variations of $[H_2O_2]_{ss}$ and hepatocyte proliferation. (A) comparison of intracellular peroxides in freshly-isolated P2 proliferating hepatocytes and differentiated P15–P90 cells. Cells were incubated with 5 μM 2′,7′-dichlorofluorescin diacetate, and live population was examined by flow cytometry. NO-dependent cytosol $[H_2O_2]_{ss}$ and $[H_2O_2]$ index, the ratio between NO-dependent (+L-arginine) and maximal (+antimycin) H_2O_2 production rates, are included. (B) Redox modulation of P2 and P15 hepatocyte proliferation (see Materials and Methods). Synchronized hepatocytes were supplemented with the different treatments (see Abbreviations) and 10% FCS for 3 days; [3H] thymidine incorporation was measured during the last 24 hours. (C) Representative flow cytometry DNA analysis of P2 hepatocytes after oxidative challenge. 2C, diploid nuclei; 4C, tetraploid nuclei. White columns represent proliferating phenotypes; grey columns represent quiescent phenotypes. Data are mean ± SE of n = 8 (treatments) and n = 16 (controls). *$P < .05$ versus the respective basal condition. P, postnatal; L-NAME, N^G-nitro-L-arginine methyl ester; NAC, N-acetyl-cysteine; GSH, glutathione; ATZ, 3-amino 1,2,4-triazole; L-Arg, L-arginine; GR-FL, green fluorescence.

To investigate mtNOS contribution, H_2O_2 production rate was measured in the presence of L-arginine alone or in addition to L-NMMA. The NO-dependent mitochondrial H_2O_2 production was undetectable in E17 mitochondria, but thereafter it progressively increased up to P30–P90, indicating a linkage with mtNOS modulation (see Fig. 3A). Furthermore, in embryos low H_2O_2 yield is cooperatively contributed by low mitochondrial complex activities and UQ content (see reactions [1] and [2] above and Table 1). A parallel increase of mtNOS, UQ, and H_2O_2 was observed in rat brain in the transit from neuroblast proliferation to neuronal differentiation.[11]

Mitochondrial Contributions to Cytosol Liver H_2O_2 Steady-State Concentration. Mitochondria is

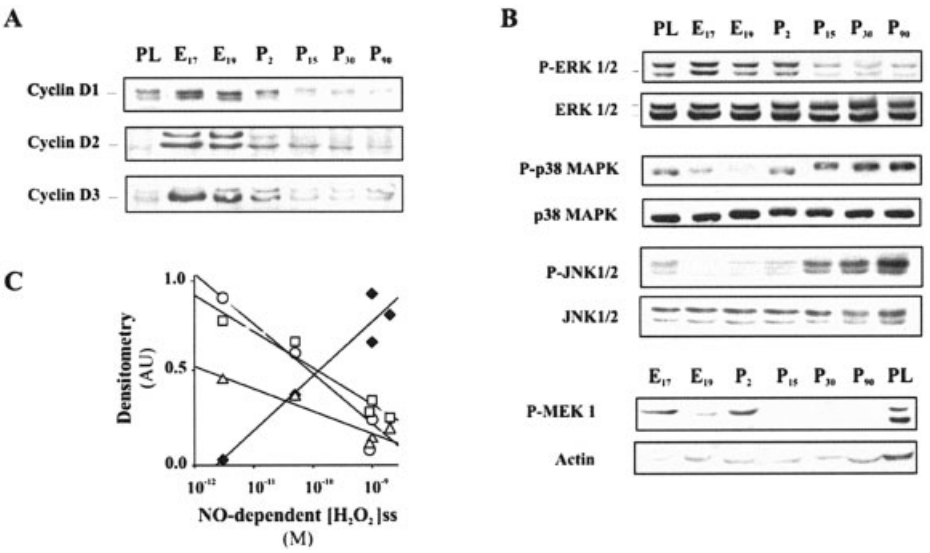

Fig. 5. Modulation of cell signaling in the developing rat liver. (A) and (B), liver homogenates (25 μg/ lane) were separated in 12% gels; T3-injected, proliferating rat liver was used as control (PL). Western blot detection of cyclins D and MAPKs was performed with specific antibodies. (C) Simple linear regression between cyclin D1, active MAPKs, and NO-dependent cytosol $[H_2O_2]_{ss}$ (cyclin D1 [○], r^2 −0.91; phospho-ERK 1 (□) and 2 [△], r^2 −0.95 and −0.96; and phospho-p38 MAPK [◆], r^2 0.76; all $P < .05$). Each point represents three independent experiments normalized to E17. E, embryonic; P, postnatal; ERK, extracellular signal–regulated kinase; MAPK, mitogen-activated protein kinase; JNK, c-Jun N-terminal kinase; MEK, MAPK kinases.

the main contributor to liver H_2O_2 steady-state concentration ($[H_2O_2]_{ss}$); only a small fraction of peroxisome-derived H_2O_2 appears to escape peroxisomal catalase.[34] Depending on matrix NO, in the steady-state condition, mitochondrial H_2O_2 production equals cytosolic H_2O_2 utilization by the two main scavenger enzymes, catalase and glutathione peroxidase. NO-dependent $[H_2O_2]_{ss}$ can be calculated according to the following equation (where $+d[H_2O_2]/dt$ is the rate of L-arginine–dependent H_2O_2 production, k_3 is the second-order rate constant for the catalase-catalyzed metabolism of H_2O_2, and k_4 is that for the glutathione peroxidase–driven reaction): [35]

$$[H_2O_2]_{ss} = + d[H_2O_2]/dt/k_3[\text{catalase}] + k_4[\text{glutathione peroxidase}] \quad (4)$$

NO-dependent $[H_2O_2]_{ss}$ was undetectable at E17 and increased by two orders of magnitude from E19 to P90 ($\approx 10^{-11}$ M to 10^{-9} M), paralleling the developmental modulation of mtNOS (Fig. 3B and C). Mn-SOD activity was similarly comodulated and well correlated with mtNOS, the net flux of H_2O_2 into cytosol and the resulted $[H_2O_2]_{ss}$ (Fig. 3 D and E).

Differential oxidant production was confirmed by flow cytometry (Fig. 4A). The dichlorofluorescin mean fluorescence ratio between P15 and P2 and adult P90 hepatocytes was about 5:15, which is in agreement with that obtained from estimated NO-dependent $[H_2O_2]_{ss}$ (≈10: 20). Thereby, the contribution of utilized NO to maximal mitochondrial H_2O_2 production (namely H_2O_2 index) markedly increased from proliferating to quiescent stages (see Fig. 4A).

These data suggest that most H_2O_2 comes from mitochondrial metabolism; at P90, NO-dependent H_2O_2 is similar to that obtained by perfusing adult rat liver.[35] Therefore, we propose a developmental grading of cytosolic $[H_2O_2]_{ss}$ as based upon a coordinated increase of mitochondrial complex activities mtNOS and Mn-SOD.

Redox Modulation of Hepatocyte Proliferation. As reported,[13] in neonatal hepatocytes there is still a synchronized high proliferation rate. We therefore attempted to mimic *ex vivo* the redox modulation of proliferation in P2 and P15 hepatocytes with low and high mtNOS content, respectively. Supplementation of synchronized P2-cultured hepatocytes with H_2O_2, catalase inhibitor 3-amino 1,2,4-triazole, or L-arginine invariably determined a dose-dependent negative modulation of cell proliferation (Fig. 4B). In contrast, decreasing cell H_2O_2 levels by controlled treatment with scavengers or NOS inhibitors such as N-acetyl-cysteine (NAC), glutathione, or N^G-nitro-L-arginine methyl ester increased proliferation rates by up to 30%. At a higher NAC concentration, a similar response was observed in more differentiated and less proliferative P15 hepatocytes with higher $[H_2O_2]_{ss}$ (see Fig. 4B). In all conditions, cell viability with Trypan blue was 98% and LDH in the culture supernatant was less than 1% of cytosol values, which indicates that at the utilized concentrations the tested compounds were not toxic for hepatocytes. No hypoploid peak representative of apoptosis was observed in the permeabilized P2 hepatocytes in the different conditions (Fig. 4C).

These results confirm that (1) hepatocyte proliferation at different developmental stages depends on a precise tissue H_2O_2 concentration and (2) in this context, proliferation correlates with liver *in vivo* developmental modulation of mitochondrial activities and mtNOS.

NO may modulate *per se* the expression of cell cycle regulatory proteins,[19] and it induces cytostasis by inhibition of cyclin D1 or by inhibition of cdc2 (cyclin E and A

pathways).[18] In accordance, NO has antimitogenic effects on cultured hepatocytes.[36]

Redox Modulation of Cell Signaling. In partial hepatectomy or injury,[37] mechanisms regulating hepatocyte proliferation rely on MAPK activation by growth factors, but fetal hepatocytes may proliferate in absence of exogenous factors with a constitutive level of MAPK activation.[38] Indeed, cyclin D1 is sufficient to promote progression of hepatocytes through G1 restriction point.[39] As has been previously reported,[13,40] cyclin D1 is up-regulated during liver proliferation (E17–P2) and almost disappears in the quiescent organ; expression of cyclins D2 and D3 followed that of cyclin D1 (Fig. 5A). However, cyclins D2 and D3 would have a lower contribution to adult liver proliferation, as shown during regeneration[41] and here after T3 treatment.

ERK activation paralleled cyclin D1 expression while p38 MAPK activation followed an inverse pattern (Fig. 5A and B). Similarly, p38 activity was reported inverse to cyclin D1 content in liver regeneration,[13] and transfection with p38-activating kinase MKK6 arrests hepatocyte growth.[15] In addition, P2 hepatocytes markedly expressed ERK1/2 upstream kinase phospho–MAPK kinases 1/2 and P90 hepatocytes did not, while phospho–c-Jun N-terminal kinase (a stress-activated kinase related to liver proliferation and apoptosis) was only detectable in the quiescent phenotypes. As referred,[42] Phospho–c-Jun N-terminal kinase increase may express both the late increase of oxidant levels and ERK decrease (Fig. 5B). Total MAPKs were not modified during development.

Liver cyclin D1 and phospho-ERKs were inverse to *in vivo* NO-dependent $[H_2O_2]_{ss}$ and H_2O_2 index; instead, this correlation was positive for p38 MAPK (Fig. 5C). Consequently, a high ERK/p38 activity ratio was representative of proliferating phenotypes; a low ERK/p38 ratio was representative of quiescent ones and was related to $[H_2O_2]_{ss}$ and liver growth. ERK/p38 ratio was considered a determinant of growth and dormancy in human cancer cells; Aguirre-Ghiso et al. showed that modulation of ERK/p38 activity by pharmacological and genetic interventions predicts the *in vivo* behavior in ≈90% of the examined cell lines. [43]

The interplay between redox status, signaling, and proliferation was analyzed by exposing P2 hepatocytes to H_2O_2, antimycin, and NAC, and/or to the ERK inhibitor U0126, p38 inhibitor SB202190, and p38 activator anisomycin. Exposure to H_2O_2 or to anisomycin markedly reduced cyclin D1 expression, leading P2 cells to the adult liver level. In these conditions, endogenous or exogenous H_2O_2 decreased ERK/p38 activity ratio, an effect equally prevented by NAC or SB202190 (Fig. 6A and B). Similarly, a marked reduction of ERK/p38 activity ratio by anisomycin or U0126 was clearly associated with the lowest hepatocyte proliferation rate (Fig. 6B and C). Likewise, SB202190 significantly increased cell proliferation by approximately 25%, and SB202190 or NAC also prevented the lowering of the proliferation rate induced by

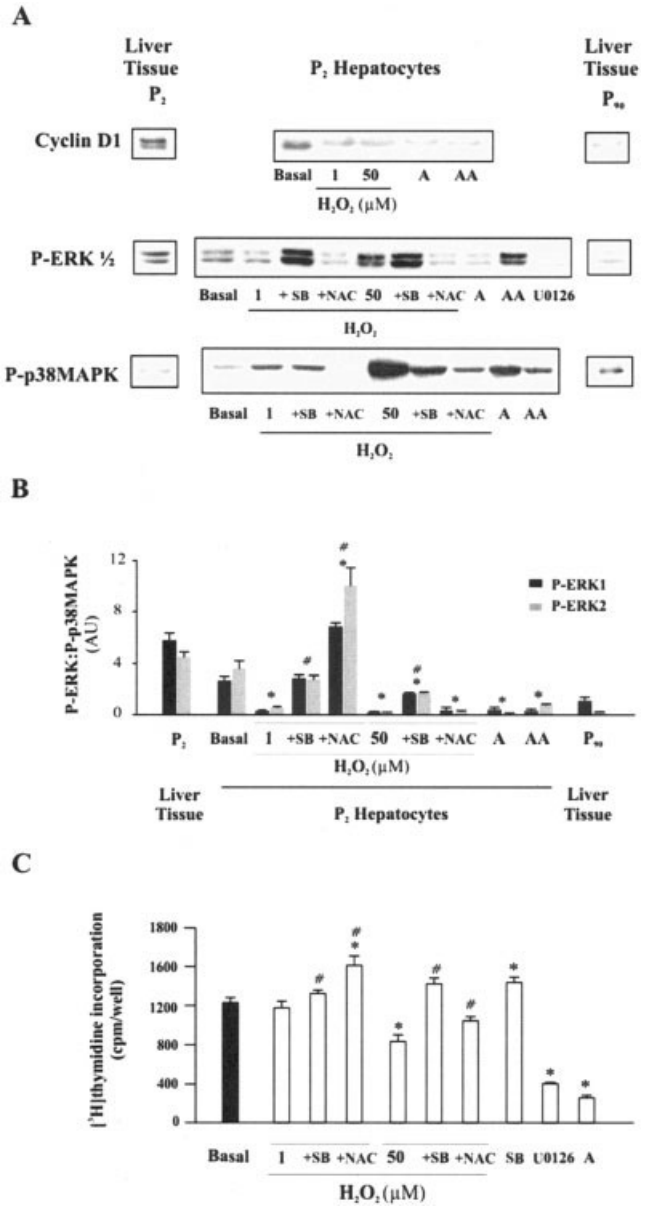

Fig. 6. Redox modulation of liver cell signaling. P2 hepatocytes were exposed to H_2O_2 alone or with 10 μM SB202190 or 0.1 mM NAC (both supplemented 2 hours before H_2O_2), 200 ng/mL anisomycin, 2 μM antimycin, and 10 μM U0126. (A) Cyclin D1 and MAPKs were detected at 2 hours and 15 minutes, respectively, by immunoblotting (50 μg/lane) in triplicate. (B) P-ERK/P-p38 MAPK ratio (densitometric measurements from three separate experiments) of the different assays is expressed. (C) P2 hepatocytes were incubated in similar conditions as those described in Fig. 4. *Different from basal condition. #Different from respective H_2O_2 concentration. $P < .05$. P, postnatal; ERK, extracellular signal–regulated kinase; A, anisomycin; AA, antimycin; SB, SB202190; NAC, N-acetyl-cysteine; MAPK, mitogen-activated protein kinase.

H_2O_2 ($p < .05$; Fig. 6B and C). These data agree with previous reports that showed that mitochondrial reactive oxygen species initiate phosphorylation of p38 in cardiomyocytes[16] and that low-level oxidative stress activates p38 and leads to growth arrest in U926 cells, an effect that is inhibited by NAC.[15]

The present results suggest that synchronized increase of mitochondrial activities, mtNOS, and $[H_2O_2]_{ss}$ operates on the balance of liver signaling pathways to drive the transition from proliferation to quiescence. In the same way, we recently reported that a critical reduction of mtNOS activity and $[H_2O_2]_{ss}$ contribute to tumoral persistent ("embryonic") behavior.[44] Further studies could confirm the contribution of mitochondrial redox signaling to the modulation of cyclins D2 and D3, which parallels cyclin D1 expression at developmental redox conditions (Fig. 5A and C) and may play a central role in liver development.

Acknowledgment: The authors thank R. Greco for her secretarial assistance, Dr. M. Barbosa for flow cytometry analysis, Dr. L. Schreier and Dr. P. Argibay for technical assistance, and Dr. E. Cadenas for helpful comments.

References

1. Fausto N, Campbell JS. The role of hepatocytes and oval cells in liver regeneration and repopulation. Mech Development 2003;120:117–130.
2. Boveris A, Poderoso J. Regulation of oxygen metabolism by nitric oxide. In: Ignarro L, ed. Nitric Oxide, Biology and Pathobiology. San Diego: Academic Press, 2000:355–368.
3. Carreras MC, Peralta JG, Converso DP, Finocchietto PV, Rebagliati I, Zaninovich AA, et al. Mitochondrial nitric oxide synthase is a final effector of thyroid-dependent modulation of oxygen uptake. Am J Physiol Heart Circ Physiol 2001;281:H2282–H2288.
4. Poderoso JJ, Carreras MC, Lisdero C, Riobó N, Schöpfer F, Boveris A. Nitric oxide inhibits electron transfer and increases superoxide radical production in rat heart mitochondria and submitochondrial particles. Arch Biochem Biophys 1996;328:85–92.
5. Giulivi C, Poderoso JJ, Boveris A. Production of nitric oxide by mitochondria. J Biol Chem 1998;273:11038–11043.
6. Ghafourifar P, Richter C. Nitric oxide synthase activity in mitochondria. FEBS Lett 1997;418:291–296.
7. Kanai AJ, Pearce L, Clemens P, Birder L, Van Bibler M, Choi S, et al. Identification of a neuronal nitric oxide synthase in isolated cardiac mitochondria using electrochemical detection. Proc Natl Acad Sci U S A 2001; 98:14126–14131.
8. Elfering SL, Sarkela TM, Giulivi C. Biochemistry of mitochondrial nitric-oxide synthase. J Biol Chem 2002;277:38079–38086.
9. Peralta JG, Finocchietto PV, Converso DP, Schöpfer F, Carreras MC, Poderoso JJ. The modulation of mitochondrial nitric oxide synthase and energy expenditure in rat cold acclimation. Am J Physiol Heart Circ Physiol 2003;284:H2375–H2383.
10. Lacza Z, Puska, M, Figueroa JP, Zhang J, Rajapakse N, Busija DW. Mitochondrial nitric oxide synthase is constitutively active and is functionally upregulated in hypoxia. Free Rad Biol Med 2001;31:1609–1615.
11. Riobo NA, Melani M, Sanjuán N, Fiszman ML, Gravielle MC, Carreras MC, et al. The modulation of mitochondrial nitric-oxide synthase activity in rat brain development. J Biol Chem 2002;277:42447–42255.
12. Huang P, Feng L, Oldham EA, Keating MJ, Plunkett W. Superoxide dismutase as a target for the selective killing of cancer cells. Nature 2000; 407:390–395.
13. Awad MM, Gruppuso PA. Cell cycle control during liver development in the rat: evidence indicating a role for cyclin D1 posttranscriptional regulation. Cell Growth Differ 2000;11:325–334.
14. Lavoie JN, L'Allemain G, Brunet A, Müller R, Pousségur J. Cyclin D1 expression is regulated positively by the p42/p44^{MAPK} and negatively by the p38/HOG^{MAPK} pathway. J Biol Chem 1996;271:20608–20616.
15. Awad MM, Enslen H, Boylan JM, Davis RJ, Gruppuso PA. Growth regulation via p38 mitogen-activated protein kinase in developing liver. J Biol Chem 2000;275:38716–38721.
16. Kurata S. Selective activation of p38 MAPK cascade and mitotic arrest caused by low level oxidative stress. J Biol Chem 2000;275:23413–23416.
17. Kulisz A, Chen N, Chandel NS, Shao Z, Schumscker PT. Mitochondrial ROS initiate phosphorylation of p38 MAP kinase during hypoxia in cardiomyocytes. Am J Physiol Lung Cell Mol Physiol 2002;282:L1324–L1329.
18. Pervin S, Singh R, Chaudhuri G. Nitric oxide-induced cytostasis and cell cycle arrest of a human breast cancer cell line (MDA-MB-231): potential role of cyclin D1. Proc Natl Acad Sci U S A 2001;98:3583–3588.
19. Tanner FC, Meier P, Greutert H, Champion C, Nabel EG, Lüscher TF. Nitric oxide modulates expression of cell cycle regulatory proteins. A cytostatic strategy for inhibition of human vascular smooth muscle cell proliferation. Circulation 2000;101:1982–1989.
20. Morais Cardoso S, Pereira C, Resende Oliveira C. Mitochondrial function is differentially affected upon oxidative stress. Free Rad Biol Med 1999;26: 3–13.
21. Pibiri M, Ledda-Columbano GM, Cossu C, Simbula G, Menegazzi M, Shinozuka H, et al. Cyclin D1 is an early target in hepatocyte proliferation induced by thyroid hormone (T3). FASEB J 2001;15:1006–1013.
22. Poderoso JJ, Lisdero C, Schöpfer F, Riobó N, Carreras MC, Cadenas E, et al. The regulation of mitochondrial oxygen uptake by redox reactions involving nitric oxide and ubiquinol. J Biol Chem 1999;274:37709–37716.
23. Herrera B, Alvarez AM, Sánchez A, Fernández M, Roncero C, Benito M, et al. Reactive oxygen species (ROS) mediates the mitochondrial-dependent apoptosis induced by transforming growth factor β in fetal hepatocytes. FASEB J 2001;15:741–751.
24. Nicoletti I, Miglioratti G, Pagliacci MC, Grignani F, Riccardi C. A rapid and simple method for measuring thymocyte apoptosis by propidium iodide staining and flow cytometry. J Immunol Methods 1991;139:271–279.
25. McCord JM, Fridovich I. The utility of superoxide dismutase in studying free radical reactions. I. Radicals generated by the interaction of sulfite, dimethyl sulfoxide, and oxygen. J Biol Chem 1969;244:6049–6065.
26. Chance B. Special methods: catalase. In: Glick D, ed. Methods of Biochemical analysis. New York: Interscience, 1954:408–424.
27. Burk RF, Nishiki K, Lawrence RA, Chance B. Peroxide removal by selenium-dependent and selenium-independent glutathione peroxidases in hemoglobin-free perfused rat liver. J Biol Chem 1978;253:43–46.
28. David H. The hepatocyte. Development, differentiation, and ageing. Exp Pathol Suppl 1985;11:1–148.
29. Streumer-Svobodova Z, Drahota Z. The development of oxidative enzymes in rat liver mitochondria. Physiol Bohemoslov 1977;26:525–534.
30. Cuezva JM, Ostronoff LK, Ricart J, López de Heredia M, Di Ligero CM, Izquierdo JM. Mitochondrial biogenesis in the liver during development and oncogenesis. J Bioenerg Biomembr 1997;29:365–367.
31. Simmonet H, Alazard N, Pfeiffer K, Gallou C, Bewroud C, Demont J, et al. Low mitochondrial respiratory chain content correlates with tumor aggressiveness in renal cell carcinoma. Carcinogenesis 2002;23: 759–768.
32. Oyanagi K, Nakamura K, Sogawa H, Tsukuzaki H, Minami R, Nakao T. A study of urea-synthesizing enzymes in prenatal and postnatal human liver. Pediatr Res 1980;14:236–241.

33. Tanaka K, Harioka T, Murachi T. Changes in contents of calpain and calpastatin in rat liver during growth. Physiol Chem Phys Med NMR 1985;17:357–363.
34. Thannickal VJ, Fanburg BL. Reactive oxygen species in cell signaling. Am J Physiol Lung Cell Mol Physiol 2000;279:L1005–L1028.
35. Boveris A, Cadenas E. Cellular sources and steady-state levels of reactive oxygen species. In: Biadasz Clerch L, Massaro DJ, eds. Oxygen, Gene Expression, and Cellular Function. New York: Marcel Dekker, 1997:1–25.
36. Dalmau M, Joaquin M, Nakamura T, Bartrons R, Gil J. Nitric oxide inhibits DNA synthesis and induces activation of poly(ADP-ribose) polymerase in cultured rat hepatocytes. Exp Cell Res 1996;228:14–18.
37. Fausto N, Laird AD, Webber EM. Liver regeneration. 2. Role of growth factors and cytokines in hepatic regeneration. FASEB J 1995;9:1527–1536.
38. Boylan JM, Gruppuso PA. Uncoupling of hepatic, epidermal growth factor-mediated mitogen-activated protein kinase activation in the fetal rat. J Biol Chem 1998;273:3784–3790.
39. Nelsen CJ, Rickheim DG, Timchenko NA, Stanley MW, Albrecht JH. Transient expression of cyclin D1 is sufficient to promote hepatocyte replication and liver growth *in vivo*. Cancer Res 2001;61:8564–8568.
40. Matsui T, Kinoshita T, Hirano T, Yokota T, Miyajima A. STAT3 down-regulates the expression of cyclin D during liver development. J Biol Chem 2002;277:36167–36173.
41. Rickheim DG, Nelsen CJ, Fassett JT, Timchenko NA, Hansen LK, Albrecht JH. Differential regulation of cyclins D1 and D3 in hepatocyte proliferation. HEPATOLOGY 2002;36:30–38.
42. Czaja MJ, Liu H, Wang Y. Oxidant-induced hepatocyte injury from menadione is regulated by ERK and AP-1 signaling. HEPATOLOGY 2003;37:1405–1413.
43. Aguirre-Ghiso JA, Estrada Y, Liu D, Ossowski L. ERK^{MAPK} activity as a determinant of tumor growth and dormancy; regulation by $p38^{SAPK}$. Cancer Res 2003;63:1684–1695.
44. Galli S, Labato MI, Bal de Kier Joffé E, Carreras MC, Poderoso JJ. Decreased mitochondrial nitric oxide synthase activity and hydrogen peroxide relate persistent tumoral proliferation to embryonic behavior. Cancer Res 2003;63:6370–6377.